Diameter dependent phonon-induced backscattering in semiconducting carbon nanotubes

Luis E. F. Foa Torres[1,2,*] and Stephan Roche[1]
[1]*CEA/DSM/DRFMC/SPSMS/GT, 17 Avenue des Martyrs, 38054 Grenoble, France*
[2]*CEA Léti-MINATEC, 17 rue des Martyrs, 38054 Grenoble, France*
(Received 1 December 2006; revised manuscript received 18 January 2007; published 10 April 2007)

We report on a many-body theoretical study of the effects of electron-(optical)phonon interaction on transport through zigzag semiconducting carbon nanotubes. We show that the interaction with $A_1(L)$ phonon mode of energy $\hbar\omega_0$ induces the opening of nonequilibrium energy gaps at $\hbar\omega_0/2$ and/or $\hbar\omega_0$ above (below) the charge neutrality point, depending on the tube diameter and phonon population. These mechanisms, which correspond to inelastic backscattering with phonon emission (absorption), are *beyond* the scope of the conventional Born-Oppenheimer and Fermi golden rule approximations.

DOI: 10.1103/PhysRevB.75.153402 PACS number(s): 73.63.Fg, 72.10.Di, 73.23.−b, 05.60.Gg

Carbon nanotubes (CNTs) are nanometer scale diameter tubes made of graphitic carbon. Since their discovery, these objects have captivated the attention of numerous researchers due to their exceptional mechanical and electrical properties.[1] In particular, the study of electronic transport in CNTs stands as a major driving force, with phenomena that include superconductivity and Luttinger liquid behavior. Besides, recent progress in the fabrication of low resistance contacts allowed the observation of ballistic electron transport in metallic[2,3] as well as in semiconducting nanotubes,[4] thus offering an outstanding arena for studying the intrinsic transport properties in low dimensionality.

However, ballistic transport is limited to the low bias regime whether at high bias a current saturation attributed to electron backscattering by optical or zone boundary phonons is observed.[4,5] Motivated by these experiments, a wealth of theoretical studies were aimed at describing the effects of electron-phonon (e-ph) interaction, most of them focused on metallic nanotubes. They include simulations based on the Boltzmann equation,[6–9] the Fermi golden rule,[10] the Kubo approach,[11] and the use of a diagonal approximation for the phonon self-energy in the self-consistent Born approximation.[12,13] In contrast, much less attention was given to semiconducting CNTs despite their prime relevance to engineer novel field-effect transistors.

While most of the theoretical approaches to e-ph interaction can only cope with perturbative effects, physics beyond ordinary perturbation theory can play a key role in these systems and may yield important modifications of both phonon and electronic band structures. Fundamental examples are the Kohn anomaly[14] and the Peierls transition.[15] In CNTs the latter is not effective enough to open an energy gap except for tubes either with a very small radius[16] or at very low temperatures ($\sim$10 K).[17] Nevertheless, based on *ab initio* calculations, Dubay *et al.*[18] found a softening of an $A_1(L)$ phonon mode in metallic tubes, not able, however, to produce a static lattice distortion. Strikingly, no softening of the $A_1(L)$ phonon mode was found for semiconducting tubes of similar diameter, suggesting that e-ph coupling is inefficient for semiconducting tubes in the diameter range explored in Ref. 18 ($d<16$ Å). In Ref. 19, by using a nonperturbative many-body treatment for the e-ph interaction in *metallic* tubes, the coupling of electrons with $A_1(L)$ phonon mode was proven to induce the opening of nonequilibrium energy gaps at $\hbar\omega_0/2$ above (below) the charge neutrality point (CNP) owing to phonon emission (absorption) activated through a bias voltage. This novel mechanism was shown to induce an onset of current saturation for bias voltages of $\sim\hbar\omega_0$.

In this Brief Report, we present a theoretical study of the effects of the interaction between electrons and $A_1(L)$ optical phonons in the transmission through $(N,0)$ *semiconducting* zigzag tubes. The observed phenomena are found to critically depend on the tube diameter. For long diameter tubes ($d>4.4$ nm, $N\geqslant 55$), two main features driven by e-ph coupling are observed: the opening of energy gaps at $\hbar\omega_0/2$ *and* $\hbar\omega_0$ above (below) the CNP due to inelastic backscattering with the emission (absorption) of one and two phonons, respectively. For tubes with $d>2.1$ nm ($N\geqslant 28$), only the second feature remains robust, while for $d\lesssim 2.1$ nm, none of these features are present, thereby suggesting that the interaction with $A_1(L)$ phonons does not play any role in this case.[20] This is in striking contrast with metallic tubes of similar radii.[19] The scaling with the tube length as well as the effect of an increase in the phonon population are also investigated. These features, which we explain as a lifting of degeneracies between e-ph Fock states due to the e-ph interaction, are beyond the scope of semiclassical treatments based on the Born-Oppenheimer[21] and Fermi golden rule approximations.[10]

Following Ref. 19, we consider an infinite CNT where the electrons interact with phonons only in a central part of length L. The Hamiltonian is $H=H_e+H_{ph}+H_{e\text{-}ph}$. The electronic part is described by a π-orbital model: $H_e=-\gamma_0\Sigma_{\langle i,j\rangle}[c_i^+c_j+\text{H.c.}]$, where c_i^+ and c_i are the electron operators for electrons at site i and $\gamma_0=2.77$ eV.[1] The phonon term is $H_{ph}=\hbar\omega_0 b^+b$, b^+ and b being the operators for the $A_1(L)$ phonons. Finally, the e-ph interaction in the central part of the tube is described through a Su-Schreiffer-Heeger Hamiltonian:[21,22]

$$H_{e\text{-}ph}=\sum_{\langle i,j\rangle}[\gamma_{i,j}^{e\text{-}ph}c_i^+c_j(b^+ + b)+\text{H.c.}], \tag{1}$$

where the e-ph matrix elements are given by $\gamma_{i,j}^{e\text{-}ph}=\alpha\sqrt{\hbar/(2m\omega_0)}\hat{\delta}_{i,j}\cdot(\vec{e}_i-\vec{e}_j)$, $\vec{e}_i$ is the phonon mode eigenvec-

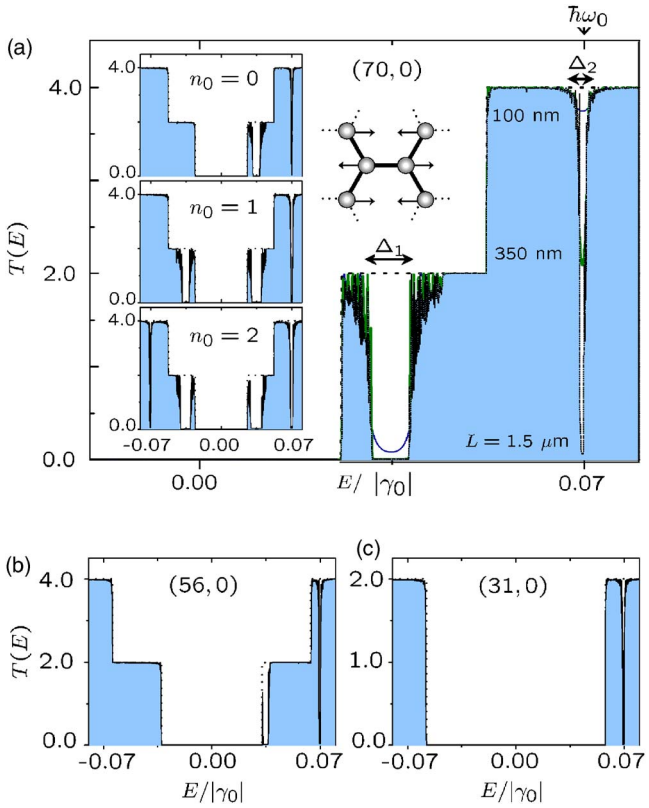

FIG. 1. (Color online) (a) Total transmission probability as a function of the energy of the incident electrons for a (70,0) tube and $n_0=0$. The dotted line corresponds to the case of vanishing e-ph interaction, the other curves are for different values of L. Inset: Same information for $n_0=0$, 1, and 2 over a broader energy range and $L=1.5$ μm. (b) and (c) show the same information as (a) for (56,0) and (31,0) tubes ($L=1.5$ μm).

tor. $\hat{\delta}_{i,j}$ is a unit vector in the bond direction and α is the e-ph coupling strength.

For the $A_1(L)$ phonon mode considered here, A- and B-type atoms move out of phase in the direction parallel to the tube axis [see scheme in Fig. 1(a)]. This gives e-ph matrix elements $\gamma_{i,j}^{\text{e-ph}}$ with values $\gamma_0^{\text{e-ph}}=-\alpha\sqrt{\hbar/(m\omega_0)}$ for bonds (i,j) that are parallel to the tube axis, and $-\gamma_0^{\text{e-ph}}\cos(\pi/3)$ for bonds (i,j) that are tilted with respect to the tube axis.[23]

To investigate quantum transport for the e-ph Hamiltonian (1), the approach introduced in Refs. 24 and 25 is used. The keystone is to write the Hamiltonian in an appropriate basis for the e-ph Fock space (a single electron plus phonons) to construct an equivalent multichannel one-body problem. To fix ideas, let us consider an electron that tunnels from a left electrode (L) to a right electrode (R), while it interacts with a single phonon mode. Then, the asymptotic states in the noninteracting electrodes can be labeled by means of two indices: (X,n), $X=L,R$ being the index corresponding to the electrode and n the number of phonons in the system. This is equivalent to a multichannel one-body problem where the asymptotic states in the e-ph Fock space include both the electronic and vibrational degrees of freedom. Each phonon mode adds a dimension to the problem. The transmission $T_{(X,n)\to(Y,m)}$ and reflection probabilities $R_{(X,n)\to(Y,m)}$ between the different channels are computed by using Green's function techniques.[26] Once these probabilities are calculated, they are used as inputs to obtain the self-consistent nonequilibrium electron distributions in the leads (at finite temperature and voltage).[27] The electronic current can be obtained from these self-consistent distributions which take into account the Pauli exclusion principle for the different competing elastic and inelastic processes.

Figure 1(a) shows the total transmission probability $T(E)=\Sigma_n T_{(L,n_0)\to(R,n)}(E)$ for a (70,0) tube as a function of the incident's electron energy E for different tube lengths L. These curves are for the case when there are initially no phonons in the system, $n_0=0$. All the energies are expressed in units of γ_0, the value of $\hbar\omega_0$ is taken as $0.07\gamma_0$,[18] and $\alpha=\alpha_0\simeq 7$ eV/Å is estimated from Ref. 28. The main features are the appearance of dips of different widths at $E\sim\hbar\omega_0/2$ and $E\sim\hbar\omega_0$ above the CNP ($E=0$) that develop into full gaps as L increases. The elastic part of the transmission almost coincides with T and is not shown in Fig. 1(a) for better visualization. Although the transmission is dominated by elastic processes, the main contributions to the reflection probability are inelastic. In particular, we observe that the transmission suppressions at $E\sim\hbar\omega_0/2$ and $E\sim\hbar\omega_0$ are complemented by an increase in the probability of *inelastic backscattering with the emission of one and two phonons*, respectively.

In the left inset of Fig. 1(a), the curve in the main frame for $L=1.5$ μm is reproduced over a broader energy range (top inset) together with those obtained when one and two phonons are already available for scattering, $n_0=1,2$ (center and bottom insets). The area under the curves are filled in blue (color online). For $n_0=1,2$, the gaps observed in the top inset are enhanced due to stimulated phonon emission. Besides, we observe that phonon absorption processes originate the opening of additional gaps at $E\sim-\hbar\omega_0/2$ and $E\sim-\hbar\omega_0$. These features correspond to *inelastic backscattering with the absorption of one and two phonons*.

What is the scaling behavior with the tube radius? As the tube radius decreases, the intrinsic semiconducting gap Δ_0 broadens. For $(N,0)$ tubes with $N<55$ ($d<4.4$ nm), $\Delta_0>\hbar\omega_0$ and the phonon-induced gap at $E\sim\hbar\omega_0/2$ disappears [see Fig. 1(b)]. For $N<28$, $\Delta_0>2\hbar\omega_0$ and the phonon-induced gap at $E\sim\hbar\omega_0$ does not manifest [see Fig. 1(c)]. Finally, we find that for tubes with diameter smaller than 2.1 nm, this longitudinal optical mode does not play any role.

To gain an understanding of these phenomena, let us consider an infinite zigzag tube in the presence of e-ph interaction. The use of a mode decomposition[29,30] for the electronic part of the Hamiltonian simplifies the analysis. The idea is to rewrite the problem on the basis that diagonalizes H_e for each layer of carbon atoms perpendicular to the tube axis. The Hilbert space can be expanded in terms of the states $|l_q\rangle$ corresponding to the different circumferential modes q ($q=0,1,\ldots,N-1$) localized at the lth layer of the tube. In the absence of static disorder, the electronic Hamiltonian H_e does not couple the different modes, and the different subbands correspond to linear chains with alternating hoppings γ_0 and $\gamma_q=2\gamma_0\cos(q\pi/N)$ and dispersion relations:

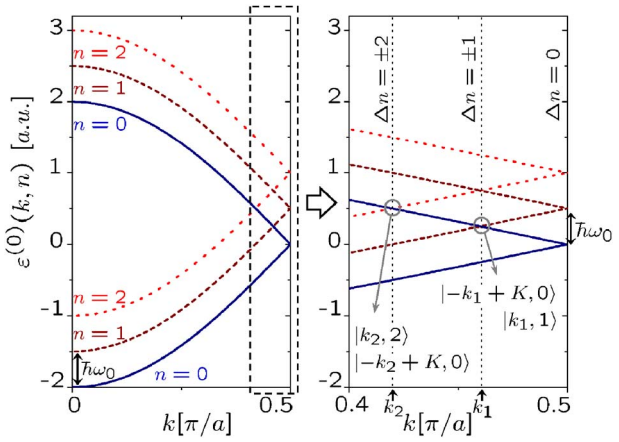

FIG. 2. (Color online) Left panel: Reduced zone scheme for the unperturbed $[H_e^{(1)}=0,\ H_{e\text{-ph}}=0]$ dispersion relations corresponding to $n=0,1,2$ for an electronic circumferential mode q. At the crossing points between these curves (see right panel), the e-ph interaction can lift the degeneracies, leading to the opening of energy gaps. The Fock states for two of these degeneracy points are indicated in the right panel.

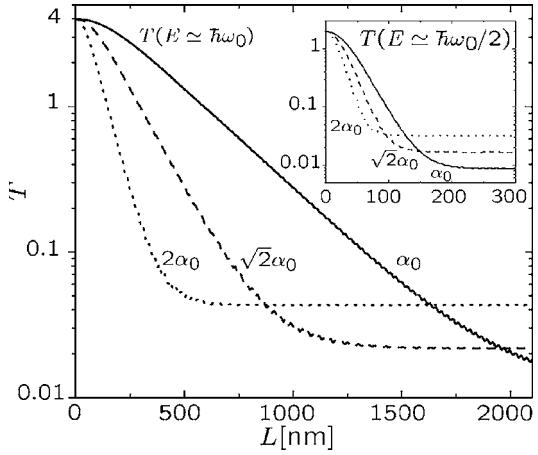

FIG. 3. Total transmission probability at $E\simeq\hbar\omega_0$ (main frame) and $E\simeq\hbar\omega_0/2$ (inset) as a function of the tube length for $n_0=0$ and $\alpha=\alpha_0,\sqrt{2}\alpha_0$ and $2\alpha_0$. The other parameters are taken as in Fig. 1(a).

$\varepsilon^{(0)}(k)=\pm\sqrt{\gamma_0^2+\gamma_q^2+2\gamma_0\gamma_q\cos(3ka_{cc}/2)}$. For metallic tubes, the massless subbands that contribute to the density of states close to the CNP correspond to $q=N/3,2N/3$.

Furthermore, the symmetry of the considered phonon mode prevents the coupling between different circumferential modes, thus giving N independent problems for each value of q. The corresponding e-ph matrix elements $\gamma^{\text{e-ph}}_{l_q,l'_q}$ have alternating values $\gamma_0^{\text{e-ph}}$ and $-\gamma_0^{\text{e-ph}}\cos(q\pi/N)$. The Fock space for the coupled e-ph system can be expanded either in terms of the basis states $\{|l_q,n\rangle=|l_q\rangle\otimes|n\rangle\}$, where $|n\rangle$ corresponds to the state with n phonons in the system, or alternatively, $\{|k,n\rangle=|k\rangle\otimes|n\rangle\}$ where $|k\rangle$ is a plane wave in mode space with wave vector k along the axis direction.

To understand the gaps in Fig. 1 as well as the scaling with the tube diameter, let us analyze a generic sub-band q. We start by writing H_e as a sum of two parts: $H_e^{(0)}$ which is the Hamiltonian for a massless subband and $H_e^{(1)}\equiv H_e-H_e^{(0)}$. The matrix elements of $H_e^{(1)}$ are proportional to the intrinsic gap of the subband ($|\gamma_0|-|\gamma_q|$) and have a two layer periodicity with associated wave vector $K=\pi/a$ ($a\equiv 3a_{cc}/4$). By neglecting $H_e^{(1)}$ and $H_{e\text{-ph}}$ in the Hamiltonian, we obtain dispersion relations $\varepsilon^{(0)}(k,n)=\langle k,n|H_e^{(0)}+H_{\text{ph}}|k,n\rangle$ as shown schematically in Fig. 2 for $n=0,1,2$ using a reduced zone. The effect of the neglected terms, $H_e^{(1)}$ and $H_{e\text{-ph}}$, are potentially stronger at the points where these curves intersect with each other (see Fig. 2, right panel). For nonvanishing $H_e^{(1)}$, there is an energy gap Δ_0 at the crossing points located at the border of the zone. The other intersection points correspond to degenerate Fock states whose phonon numbers are different, $\Delta n=\pm1,\pm2$, and are located at electronic energies $\pm\hbar\omega_0/2$ and $\pm\hbar\omega_0$. Their degeneracy can only be lifted by the e-ph interaction term.

The magnitude of Δ_0, which is of topological origin and not related to e-ph coupling, has a direct influence on the crossing points with $\Delta n=\pm1,\pm2$. For $\Delta_0>\hbar\omega_0$, there are no degeneracies with $\Delta n=\pm1$, while those with $\Delta n=\pm2$ are absent for $\Delta_0>2\hbar\omega_0$. When present, the degeneracies between Fock states differing in one phonon will be lifted due to the two-layer spatial periodicity of the e-ph interaction ($\langle\pm k_1\mp K,n_0|H_{e\text{-ph}}|\pm k_1,n_0+1\rangle\neq0$), leading to a gap $\Delta_1(n_0)\simeq2\sqrt{n_0+1}|\gamma_0^{\text{e-ph}}|(1+|\cos(q\pi/N)|)$. On the other hand, the degeneracies involving $\Delta n=\pm2$ are also lifted by the two-phonon processes, giving rise to a gap $\Delta_2(n_0)\simeq(1/4)[\Delta_1(n_0)/\hbar\omega_0](\Delta_0/\hbar\omega_0)\Delta_1(n_0+1)$.[31] These predictions are in quantitative agreement with the prior numerical results.

Note also that $\Delta_2(n_0)$ scales as $(n_0+1)^2$, while $\Delta_1(n_0)\propto(n_0+1)$ and therefore the two-phonon gap is more sensitive to changes in the phonon population (see Fig. 1 inset). The results of Ref. 19 for metallic tubes are a particular case of those presented before (we remark that Δ_2 vanishes for a massless subband).

The scaling of the main features observed in Fig. 1(a) with the tube length is further explored in Fig. 3. The total transmission probabilities at the energies corresponding to the center of the one- and two-phonon emission gaps ($E\sim\hbar\omega_0/2,\hbar\omega_0$, the exact value being α dependent) are shown as a function of the tube length L. There is a range of L where the transmission at both gaps exhibit an exponential decay due to tunneling followed by a saturation regime. These saturations are due to phonon-assisted tunneling through the gap and are proportional to α^2. The decay corresponding to energies around the first gap is of the same nature as the one observed for metallic tubes,[19] that is, $T(E\sim\hbar\omega_0/2)\propto\exp(-L/\xi_1)$, with $\xi_1\propto1/\Delta_1\propto1/\alpha$. In contrast, the exponential decay for energies close to the second gap is $T(E\sim\hbar\omega_0)\propto\exp(-L/\xi_2)$, where $\xi_2\propto1/\Delta_2\propto1/\alpha^2$. For $\alpha=\alpha_0$, we obtain $\xi_1\simeq22$ nm and $\xi_2\simeq3\times10^2$ nm. Note that the above exponential scaling of T with L jeopardizes the interpretation in terms of a diffusive regime governed by some inelastic scattering length, in contrast to common belief.[5]

To conclude, we remark that, as discussed in Ref. 19, the reported phonon-induced energy gaps will develop in the

out-of-equilibrium regime and are activated at high bias voltage. The calculation of current-voltage characteristics requires, however, a detailed modeling of contact and electrostatic effects, which is left for future study.

This work was supported by the Carnot Institute at LETI and "Transnanofils" ACI and "ACCENT" ANR/PNANO projects.

*Electronic address: luisfoa@gmail.com

[1] R. Saito, G. Dresselhaus, and M. S. Dresselhaus, *Physical Properties of Carbon Nanotubes* (Imperial College Press, London, 1998).

[2] W. Liang, M. Bockrath, D. Bozovic, J. H. Hafner, M. Tinkham, and H. Park, Nature (London) **411**, 665 (2001).

[3] J. Kong, E. Yenilmez, T. W. Tombler, W. Kim, H. Dai, R. B. Laughlin, L. Liu, C. S. Jayanthi, and S. Y. Wu, Phys. Rev. Lett. **87**, 106801 (2001).

[4] A. Javey, J. Guo, Q. Wang, M. Lundstrom, and H. Dai, Nature (London) **424**, 654 (2003).

[5] Z. Yao, C. L. Kane, and C. Dekker, Phys. Rev. Lett. **84**, 2941 (2000).

[6] V. Perebeinos, J. Tersoff, and P. Avouris, Phys. Rev. Lett. **94**, 086802 (2005).

[7] M. A. Kuroda, A. Cangellaris, and J.-P. Leburton, Phys. Rev. Lett. **95**, 266803 (2005).

[8] M. Lazzeri and F. Mauri, Phys. Rev. B **73**, 165419 (2006).

[9] M. Z. Kauser and P. P. Ruden, Appl. Phys. Lett. **89**, 162104 (2006).

[10] M. Lazzeri, S. Piscanec, F. Mauri, A. C. Ferrari, and J. Robertson, Phys. Rev. Lett. **95**, 236802 (2005).

[11] S. Roche, J. Jiang, F. Triozon, and R. Saito, Phys. Rev. Lett. **95**, 076803 (2005).

[12] A. Svizhenko and M. P. Anantram, Phys. Rev. B **72**, 085430 (2005).

[13] S. O. Koswatta, S. Hasan, M. S. Lundstrom, M. P. Anantram, and D. E. Nikonov, Appl. Phys. Lett. **89**, 023125 (2006).

[14] S. Piscanec, M. Lazzeri, F. Mauri, A. C. Ferrari, and J. Robertson, Phys. Rev. Lett. **93**, 185503 (2004); S. Piscanec, M. Lazzeri, J. Robertson, A. C. Ferrari, and F. Mauri, Phys. Rev. B **75**, 035427 (2007).

[15] J. W. Mintmire, B. I. Dunlap, and C. T. White, Phys. Rev. Lett. **68**, 631 (1992); R. Saito, M. Fujita, G. Dresselhaus, and M. S. Dresselhaus, Phys. Rev. B **46**, 1804 (1992); K. Harigaya and M. Fujita, *ibid.* **47**, 16563 (1993).

[16] D. Connetable, G.-M. Rignanese, J.-C. Charlier, and X. Blase, Phys. Rev. Lett. **94**, 015503 (2005).

[17] M. T. Figge, M. Mostovoy, and J. Knoester, Phys. Rev. Lett. **86**, 4572 (2001).

[18] O. Dubay, G. Kresse, and H. Kuzmany, Phys. Rev. Lett. **88**, 235506 (2002); O. Dubay and G. Kresse, Phys. Rev. B **67**, 035401 (2003).

[19] L. E. F. Foa Torres and S. Roche, Phys. Rev. Lett. **97**, 076804 (2006); Appl. Phys. A: Mater. Sci. Process. **86**, 283 (2007).

[20] For small tube radius, the Schottky barrier effects become stronger and may reduce the effectiveness of e-ph backscattering; see Z. Chen, J. Appenzeller, J. Knoch, Y. Lin, and P. Avouris, Nano Lett. **5**, 1497 (2005).

[21] W. P. Su, J. R. Schrieffer, and A. J. Heeger, Phys. Rev. Lett. **42**, 1698 (1979).

[22] G. D. Mahan, Phys. Rev. B **68**, 125409 (2003).

[23] Note that a $1/\sqrt{2}$ factor was missing in the expression given for $\gamma_0^{\text{e-ph}}$ in Ref. 19.

[24] E. V. Anda, S. S. Makler, H. M. Pastawski, and R. G. Barrera, Braz. J. Phys. **24**, 330 (1994).

[25] J. Bonča and S. A. Trugman, Phys. Rev. Lett. **75**, 2566 (1995).

[26] L. E. F. Foa Torres, H. M. Pastawski, and S. S. Makler, Phys. Rev. B **64**, 193304 (2001).

[27] E. G. Emberly and G. Kirczenow, Phys. Rev. B **61**, 5740 (2000).

[28] D. Porezag, T. Frauenheim, T. Kohler, G. Seifert, and R. Kaschner, Phys. Rev. B **51**, 12947 (1995).

[29] L. Balents and M. P. A. Fisher, Phys. Rev. B **55**, R11973 (1997).

[30] N. Mingo, Liu Yang, Jie Han, and M. P. Anantram, Phys. Status Solidi B **226**, 79 (2001).

[31] Δ_2 can be obtained by considering a block of the Hamiltonian corresponding to the states $|\pm k_2 \mp K, n_0\rangle$, $|\pm k_2, n_0+1\rangle$, $|\pm k_2 \mp K, n_0+1\rangle$, and $|\pm k_2, n_0+2\rangle$. The first and the last states are degenerate and the remaining two serve as intermediate states that connect them, removing the degeneracy. Direct transitions between the first (second) and third (fourth) states are neglected.